Physics of Plasmas

Advances in simulations of moving striations in DC discharges of noble gases

Cite as: Phys. Plasmas **26**, 104501 (2019); https://doi.org/10.1063/1.5121846
Submitted: 29 July 2019 . Accepted: 24 September 2019 . Published Online: 08 October 2019

Robert R. Arslanbekov, and Vladimir I. Kolobov

Physics of Plasmas BRIEF COMMUNICATION scitation.org/journal/php

Advances in simulations of moving striations in DC discharges of noble gases

Cite as: Phys. Plasmas **26**, 104501 (2019); doi: 10.1063/1.5121846
Submitted: 29 July 2019 · Accepted: 24 September 2019 ·
Published Online: 8 October 2019

Robert R. Arslanbekov[1] and Vladimir I. Kolobov[1,2,a)]

AFFILIATIONS

[1]CFD Research Corporation, Huntsville, Alabama 35806, USA
[2]The Center for Space Plasma and Aeronomic Research, University of Alabama in Huntsville, Huntsville, Alabama 35899, USA

[a)]E-mail: vladimir.kolobov@cfdrc.com

ABSTRACT

We describe the results of two-dimensional self-consistent simulations of moving striations in DC discharges of noble gases for both diffuse and constricted plasma regimes. We use a fluid plasma model capturing key physics and change only one control parameter (volume recombination rate) to describe both the diffuse and constricted plasma. The newly developed implicit coupled plasma solver with an adaptive Cartesian mesh enables us to obtain for the first time the two-dimensional structure of the entire cathode-to-anode discharge and self-excited nonlinear ionization waves in the constricted plasmas. The results are in agreement with the previously developed linear theory of striations in constricted discharges.

Plasma stratification is often observed in glow discharges of atomic and molecular gases.[1] Striations also occur in Particle-in-Cell (PIC) simulations of plasmas in different gases and gas mixtures.[2,3] Plasma stratification, as an example of self-organization at the kinetic level, remains a great challenge for understanding the physics of gas discharges.[4]

Although substantial progress has been made in uncovering the nature of striations (ionization waves) in DC discharges of noble gases,[5,6] only one type of striation has been successfully reproduced in self-consistent computer simulations of an Argon discharge.[7] This type of striation is observed in DC discharges of noble gases at low pressures and high currents, near the so-called Pupp boundary in the (pR, i/R) diagram of different plasma states in noble gases (here, p is the gas pressure, R is the radius of discharge tube, and i is the discharge current).

Recently, striations in high-pressure discharges of noble gases have been studied in experiments[8] and numerical modeling.[9] Under these conditions, the positive column plasma is constricted, and the striations are two-dimensional, i.e., they exhibit substantial changes in the radial distribution of plasma parameters over the wavelength. An analytical model of two-dimensional ionization waves in the constricted discharges of noble gases was developed in Ref. 10. This model was used in Ref. 9 for the numerical analysis of stability of positive column plasma with respect to two-dimensional wave perturbations. It was confirmed that the main mechanism of plasma stratification of the constricted positive column is the nonlinear dependence of the ionization rate with respect to electron density, whereas gas heating plays a secondary role.

Nowadays, it is well-known that plasma of DC discharges in noble gases is stratified over a wide range of gas pressures and discharge currents. Several types of striations exist depending on specific values of pR and i/R. The discharge conditions of our interest here correspond to relatively high currents where Coulomb interactions among electrons influence the shape of the electron distribution function (EDF). Under these conditions, the plasma is partially ionized and collisional; the charged particles are generated via direct or stepwise ionization by electrons and either lost at the wall by the ambipolar diffusion (at low pR) or recombine in the volume (at high pR). There is a boundary (first discovered by Pupp), which separates the stratified and nonstratified plasma states on the (pR, i/R) map. The amplitude of moving striations decreases gradually by crossing the Pupp boundary with increasing discharge current.

A minimal plasma model describing striations near the Pupp boundary was introduced in Ref. 10. The model consists of the balance equation for plasma density and the current conservation under quasi-neutral conditions. The current contains the drift and diffusion components. The ionization rate is a strong function of the plasma density under conditions of interest. This nonlinear dependence of the ionization rate on plasma density as well as the presence of the volume recombination was shown to be the main cause of constriction and stratification of the positive column plasma.

In the present paper, in addition to solving the drift-diffusion equations for electrons and ions, we solve the electron energy

transport equation to account for the thermal conductivity of electrons and the related ionization nonlocality and assume the ionization rate as a function of local electron temperature. Also, we solve the Poisson equation for the electric field and can describe the entire structure of glow discharges including near-electrode phenomena,

$$\nabla \cdot \varepsilon\epsilon = e(n_e - n_i), \tag{1}$$

$$\frac{\partial n_e}{\partial t} - \nabla \cdot \mathbf{\Gamma}_e = n_e \nu_i(n_e, \varepsilon) - \beta n_e n_i, \tag{2}$$

$$\frac{\partial n_i}{\partial t} - \nabla \cdot \mathbf{\Gamma}_i = n_e \nu_i(n_e, \varepsilon) - \beta n_e n_i, \tag{3}$$

$$\frac{\partial (n_e \varepsilon)}{\partial t} - \nabla \cdot \mathbf{H}_e = e\mathbf{E} \cdot \mathbf{\Gamma}_e - n_e \sum_r K_r \Delta\varepsilon_r. \tag{4}$$

The electron and ion fluxes, $\mathbf{\Gamma}_e$ and $\mathbf{\Gamma}_i$, contain the drift and diffusion components. The electron energy flux is defined as $\mathbf{H}_e = 5\varepsilon\mathbf{\Gamma}_e/3$. The ionization frequency, $\nu_i(n_e, \varepsilon)$, is a function of mean electron energy (temperature) and also depends on the plasma density, which is the main cause of plasma stratification under conditions of interest in the present paper. The volume recombination rate β was varied to study the transition between diffuse and constricted discharges.

The details of solving Eqs. (1)–(4) using an explicit method with an adaptive Cartesian mesh (ACM) are described in Ref. 11. In the present paper, we use a recently developed fully coupled implicit solver. For this solver, Eqs. (1)–(4) are discretized in time using the first-order accuracy scheme and in space using the Finite Volume method. The resulting set of nonlinear equations is solved using the full Newton iteration scheme with appropriately constructed Jacobian matrices. The Jacobian block-diagonal matrix for the nonlinear Newton scheme was derived based on the ACM-adapted exponential (Scharfetter-Gummel) scheme for the drift-diffusion transport of electrons and ions and for the energy transport of electrons. The Newton iteration proceeds by stacking all the equations into one vector. The Jacobian of this vector with respect to the independent variables is derived analytically and computed for the ACM. The resulting linear system is solved using a linear iterative solver. We use the Conjugate Gradient Squared (CGS)-type iterative method with preconditioning by incomplete decomposition. The time step for the implicit plasma solver is defined from the condition of good convergence of the nonlinear iteration scheme. The details of the implementation, as well as a comparison of weak and strong points of explicit and implicit approaches, are described elsewhere.[12]

Simulations were performed for a rectangular box with dimensions 2×14 cm, which correspond to a tube of radius $R = 1$ cm and length $L = 14$ cm. The anode was grounded, and voltage was applied to the cathode through a simple RC external circuit with a small capacitance (so that it does not affect the solution) and some resistance to control the plasma density. The boundary conditions at $y = \pm 1$ cm correspond to dielectric walls. The electric potential at the dielectric walls was calculated from the local surface charge, which evolved in time based on electron and ion fluxes.

The key mechanism of plasma stratification under conditions of interest is the nonlinear dependence of the ionization rate on plasma density, which appears due to two factors: Maxwellization of the EDF by Coulomb interactions among electrons and stepwise ionization. Instead of solving the local Boltzmann equation for calculating the EDF and the ionization rate (as in Ref. 7), we here used a simple approximation for the ionization frequency in the following form:

$$\nu_i(n_e, \varepsilon) = \nu_0 \exp(-\varepsilon_0/\varepsilon) \begin{cases} \exp(n_e/n_0), & n_e < n_1, \\ \exp(n_1/n_0), & n_e > n_1, \end{cases} \tag{5}$$

where n_0 controls the rate of the nonlinear dependence and n_1 defines the saturation value. The dependence of the ionization frequency on electron temperature is assumed in the standard Arrhenius-type form with a parameter ε_0 corresponding to Argon gas. In future work, we plan to use the local Boltzmann solver and include the transport of excited metastable atoms for quantitative description of plasma stratification and the shape of the Pupp boundary.

A relatively high initial plasma density was used because we were not interested in the details of the gas breakdown process. The value of resistance R_c of the circuit was selected to maximize the amplitude of striations. We have observed that the striations exist only in a certain range of plasma densities (resistor or current values), where the nonlinear dependence of the ionization rate was substantial [n_e close to n_0 in Eq. (5)].

Figure 1 shows calculated dynamics of electron density in the middle of discharge, at $x = L/2$, $y = 0$. The time step for these simulations is about 2 ns. After an initial transient process, time-periodic oscillations of the plasma density are observed at this point, which correspond to moving striations. It is seen that the duration of the transient process and the frequency of the established oscillations depend strongly on the value of β, which corresponds to different gas pressures. The movies available on the journal website show detailed dynamics of the discharge development in the three cases. The first case corresponds to a diffuse voltage, the second case corresponds to a constricted discharge, and the third case is an intermediate case.

In the diffuse discharge, striations originate in the cathode region and gradually propagate toward the anode (Multimedia view). However, they actually propagate toward the cathode, which corresponds to the backward waves (with the group and phase velocities in

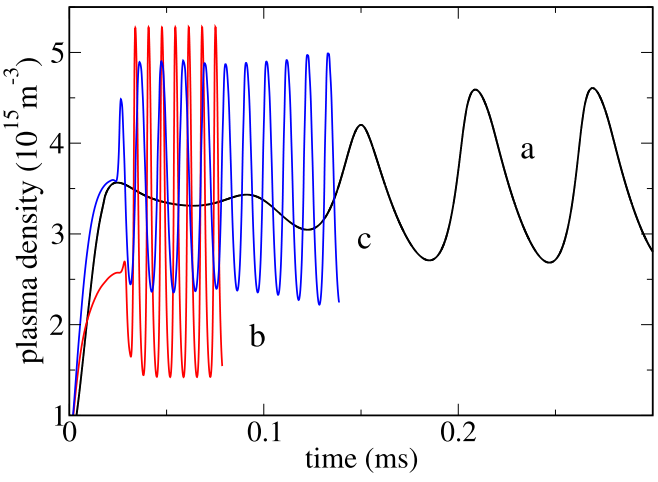

FIG. 1. Time evolution of electron density in the middle of discharge tube, at $x = L/2$, $y = 0$ for different volume recombination rates [β = 0 (a), 2.5 × 10^{-10} (b), and 10^{-10} m^{-3} s^{-1} (c)].

opposite directions), well known from the analytical theory of small-amplitude striations under these conditions.

A similar picture is observed in the constricted discharge [Multimedia view (constricted)]. The radius of the constricted plasma column is smaller than R and changes over the striation wavelength during the wave propagation. This agrees well with the reported experimental observations of the striations in constricted discharges.

A different picture of striation development is observed in the third case. The movie (Multimedia view) demonstrates that the striations originating from both sides (cathode and anode) gradually propagate toward the opposite side until they meet somewhere in the middle of the discharge tube and then start moving toward the cathode. Such a behavior was actually observed in experiments under certain conditions.[13]

Figure 2 shows an instantaneous distribution of the electron density and adapted computational mesh. A well-known structure is observed with a peak of plasma density in the negative glow inside the cathode region, a stratified positive column, and the anode region with a lower plasma density. In the diffuse discharge, the axial spatial period of striations is about the tube diameter.

In the constricted discharge, the length of striations is much smaller compared to that in the diffuse case, and it reflects the smaller radius of the constricted positive column. The radius of the plasma column increases near the electrodes. The shape of the negative glow corresponds to an abnormal discharge with current covering the entire cathode surface. The dynamically adaptive mesh helps resolving the plasma structure with a minimal number of cells for maximal efficiency. The bottom part of Fig. 2 shows an instantaneous mesh structure for the constricted discharge. The mesh adaptation criterion in the presented case is based on plasma density (to well resolve the regions with high density gradients), as well as on the magnitude of the electric field (to resolve accurately the cathode sheath region). The corresponding movie illustrates the mesh adaptation dynamics (Multimedia view).

Figure 3 shows spatial distributions of the normalized electric field, electron density, and temperature on the axis of the diffuse (left) and constricted (right) discharges. In the diffuse discharge, the maximal value of the electric field is observed near the maximal gradient of plasma density, which corresponds to the dominance of the ambipolar component of the electric field with respect to the conduction component. The maximal value of the electron temperature is shifted toward the cathode with respect to plasma density, which corresponds to propagation of striations toward the cathode. Striations are nonlinear, but no electric field reversal is observed for these conditions.

In the constricted discharge, the maximal value of the electric field is observed again near the point of the maximal plasma gradient of plasma density, which corresponds to the dominance of the ambipolar field with respect to the conduction field. The field is close to zero where the plasma density on the axis reached the maximum value, which is in good agreement with the two-dimensional theory of striations in constricted discharges.[10] The maximal value of the electron temperature is shifted toward the cathode with respect to plasma density, which corresponds to propagation of striations toward the cathode. The electric field changes its sign between the maximum of plasma density and the maximum of electron temperature. This corresponds to highly nonlinear striations under these conditions.

Figure 4 shows radial distributions of normalized electron and ion densities in two phases of striation corresponding to the maximal

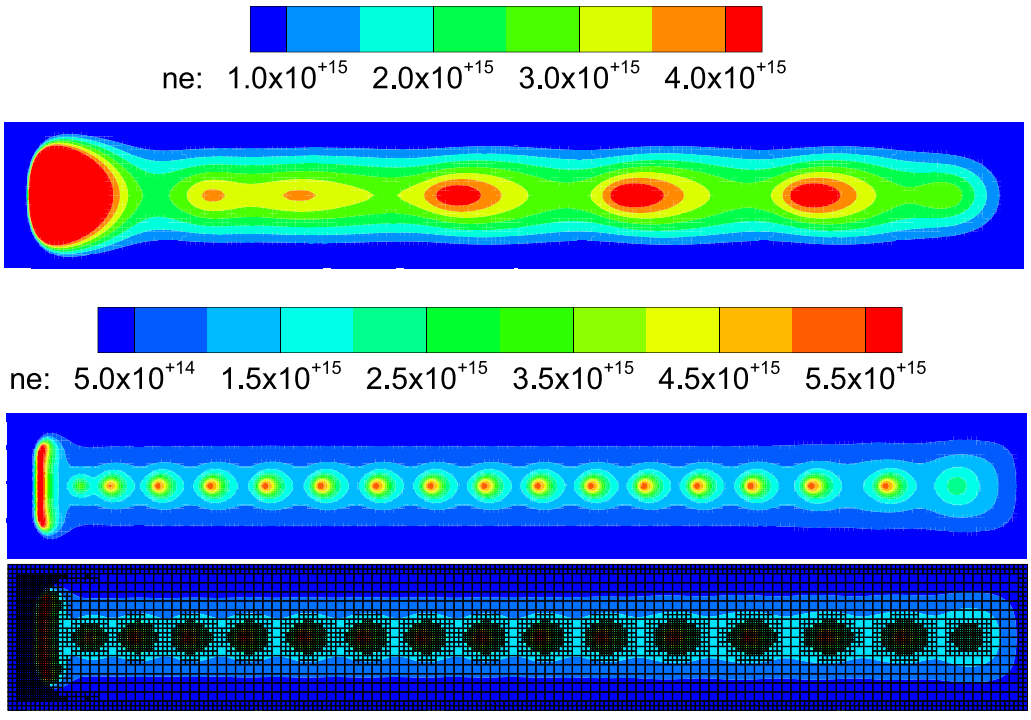

FIG. 2. Instantaneous spatial distribution of electron density for the diffuse discharge (top) and constricted discharge. The bottom picture shows the adapted Cartesian mesh. Multimedia views: https://doi.org/10.1063/1.5121846.1; https://doi.org/10.1063/1.5121846.2; https://doi.org/10.1063/1.5121846.3; https://doi.org/10.1063/1.5121846.4

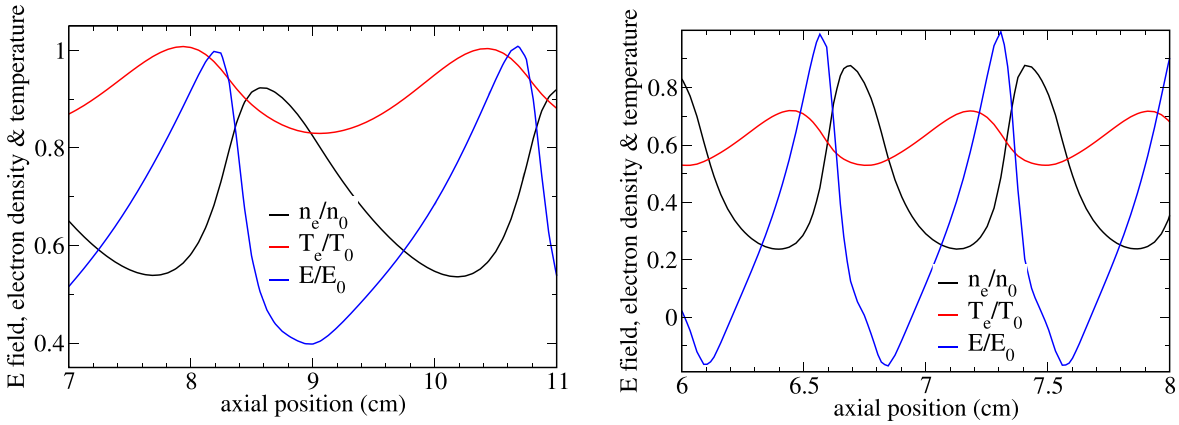

FIG. 3. Axial distributions of the normalized electric field, electron density, and temperature in the diffuse (left) and constricted (right) discharges.

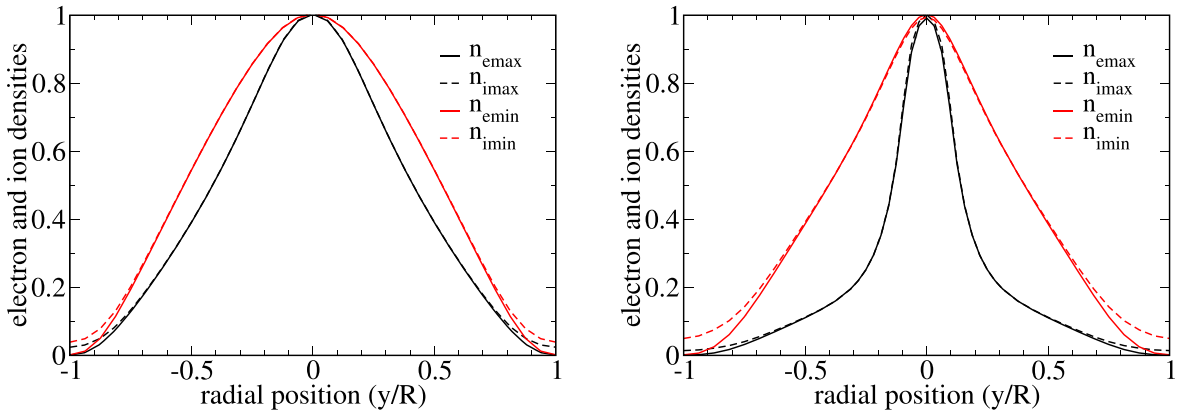

FIG. 4. Radial distributions of normalized electron and ion densities in two phases of striation corresponding to the maximal and minimal densities on the axis in the diffuse (left) and constricted (right) plasma.

and minimal densities on the axis. The space-charge sheath occupies a small fraction of the tube radius near the boundary. In the diffuse discharge (left), the radial distribution of plasma densities changes weakly. In the constricted discharge (right), the radial distribution of plasma density changes substantially over the striation wavelength. The radius of plasma has the minimum at the point of maximal plasma density on the axis, which is in good agreement with the two-dimensional theory of striations in constricted discharges.[10]

In summary, we have performed for the first time two-dimensional self-consistent simulations of self-excited moving striations in a constricted DC discharge of a noble gas using a fluid plasma model capturing key physics. The developed implicit coupled plasma solver with ACM has made such simulations possible. Simulations were performed for the entire structure of the discharge including the cathode and anode regions and describe qualitatively all the key features of the moving striations that have been observed in noble gases near the Pupp boundary. In particular, by gradually increasing the volume recombination coefficient, we have observed qualitatively a transition from diffuse to constricted discharge and analyzed the properties of striations in the diffuse and constricted column. By changing the resistance of the external circuit, we observed that striations exist only over a certain range of plasma densities (discharge currents). The results of simulations confirm that the main mechanism of plasma stratification under these conditions is associated with the nonlinear dependence of the ionization rate on plasma density, in agreement with the previously developed models of plasma stratification and constriction in noble gases at low and high gas pressures. By properly selecting the ionization and recombination rates as functions of gas pressures and plasma densities, we expect to obtain a quantitative description of the striations near the Pupp boundary in our future work.

This work was partially supported by the NSF EPSCoR Project No. OIA-1655280 "Connecting the Plasma Universe to Plasma Technology in AL: The Science and Technology of Low-Temperature Plasma."

REFERENCES

[1]V. I. Kolobov, "Glow discharges: Stratification," in *Encyclopedia of Plasma Technology* (Taylor & Francis, 2017).
[2]Y.-X. Liu, I. Korolov, E. Schüngel, Y.-N. Wang, Z. Donkó, and J. Schulze, Plasma Sources Sci. Technol. **26**, 055024 (2017).

[3]E. Kawamura, M. A. Lieberman, and A. J. Lichtenberg, Phys. Plasmas **25**, 013535 (2018).
[4]V. I. Kolobov and V. A. Godyak, Phys. Plasmas **26**, 060601 (2019).
[5]V. I. Kolobov, J. Phys. D: Appl. Phys. **39**, R487 (2006).
[6]Y. B. Golubovskii, V. O. Nekuchaev, and A. Y. Skoblo, Tech. Phys. **59**, 1787 (2014).
[7]R. R. Arslanbekov and V. I. Kolobov, IEEE Trans. Plasma Sci. **33**, 354 (2005).
[8]Y. B. Golubovskii, A. V. Siasko, D. V. Kalanov, and V. O. Nekuchaev, Plasma Sources Sci. Technol. **27**, 085009 (2018).
[9]Y. B. Golubovskii, S. Valin, E. Pelyukhova, and V. O. Nekuchaev, Plasma Sources Sci. Technol. **28**, 045015 (2019).
[10]Y. B. Golubovskii, V. I. Kolobov, and L. D. Tsendin, Sov. Phys. - Tech. Phys. **31**, 31 (1986).
[11]V. I. Kolobov and R. R. Arslanbekov, J. Comput. Phys. **231**, 839 (2012).
[12]R. R. Arslanbekov and V. I. Kolobov, "Implicit fluid plasma solver with adaptive mesh refinement," in XXXIV ICPIG & ICRP-10, Sapporo, Hokkaido, Japan, July 14–19, 2019.
[13]Y. B. Golubovskii and V. O. Nekuchaev, Sov. Phys. - Tech. Phys. **527**, 549 (1982).